HHS Public Access

Author manuscript

Mechanobiol Med. Author manuscript; available in PMC 2024 December 23.

Published in final edited form as:

Mechanobiol Med. 2024 December ; 2(4): . doi:10.1016/j.mbm.2024.100080.

Low intensity mechanical signals promote proliferation in a cell-specific manner: Tailoring a non-drug strategy to enhance biomanufacturing yields

M. Ete Chan[a,1], **Christopher Ashdown**[a,b,1], **Lia Strait**[a], **Sishir Pasumarthy**[a], **Abdullah Hassan**[a], **Steven Crimarco**[a], **Chanpreet Singh**[a], **Vihitaben S. Patel**[a], **Gabriel Pagnotti**[c], **Omor Khan**[d], **Gunes Uzer**[d], **Clinton T. Rubin**[a,e,*]

[a]Department of Biomedical Engineering, College of Engineering and Applied Sciences, Renaissance School of Medicine, Stony Brook University, Stony Brook, NY, 11794-5280, USA

[b]Medical Scientist Training Program, Renaissance School of Medicine, Stony Brook University, Stony Brook, NY, 11794, USA

[c]Department of Endocrine Neoplasia and Hormonal Disorders, MD Anderson Cancer Center, Houston, TX, 77030, USA

[d]Department of Mechanical and Biomedical Engineering, College of Engineering, Boise State University, Boise, ID, 83725-205, USA

[e]Center for Biotechnology, New York State Center for Advanced Technology in Medical Biotechnology, Stony Brook University, Stony Brook, NY, 11794-5281, USA

Abstract

Biomanufacturing relies on living cells to produce biotechnology-based therapeutics, tissue engineering constructs, vaccines, and a vast range of agricultural and industrial products. With the escalating demand for these bio-based products, any process that could improve yields and shorten outcome timelines by accelerating cell proliferation would have a significant impact across the discipline. While these goals are primarily achieved using *biological* or *chemical* strategies, harnessing cell mechanosensitivity represents a promising – albeit less studied – *physical* pathway

*Corresponding author. Rm 217, Stony Brook University, Stony Brook, NY, 11794-5281, USA. Clinton.rubin@stonybrook.edu (C.T. Rubin).

[1]these authors share co-first authorship.

Ethical statement

This study does not contain any studies with human or animal subjects performed by any of the authors.

CRediT authorship contribution statement

M. Ete Chan: Writing – original draft, Supervision, Investigation. **Christopher Ashdown:** Writing – review & editing, Validation, Methodology, Investigation, Formal analysis. **Lia Strait:** Investigation. **Sishir Pasumarthy:** Methodology, Investigation. **Abdullah Hassan:** Investigation. **Steven Crimarco:** Investigation. **Chanpreet Singh:** Investigation. **Vihitaben S. Patel:** Investigation. **Gabriel Pagnotti:** Investigation. **Omor Khan:** Methodology. **Gunes Uzer:** Writing – review & editing, Writing – original draft, Supervision, Methodology, Investigation, Formal analysis, Conceptualization. **Clinton T. Rubin:** Writing – review & editing, Writing – original draft, Supervision, Project administration, Methodology, Investigation, Funding acquisition, Formal analysis, Conceptualization.

Declaration of competing interest

CTR has several issued and pending patents on the use of low intensity vibration and extremely low magnitude mechanical signals to promote cell proliferation and differentiation, both *in vitro* and *in vivo*. He is also the founder of Lahara Bio and Marodyne Medical. No other authors have any conflicts to declare.

to promote bioprocessing endpoints, yet identifying which mechanical parameters influence cell activities has remained elusive. We tested the hypothesis that mechanical signals, delivered non-invasively using low-intensity vibration (LIV; <1 g, 10–500 Hz), will enhance cell expansion, and determined that any unique signal configuration was not equally influential across a range of cell types. Varying frequency, intensity, duration, refractory period, and daily doses of LIV increased proliferation in Chinese Hamster Ovary (CHO)-adherent cells (+79% in 96 hr) using a particular set of LIV parameters (0.2 g, 500 Hz, 3 × 30 min/d, 2 hr refractory period), yet this same mechanical input *suppressed* proliferation in CHO-suspension cells (−13%). Another set of LIV parameters (30 Hz, 0.7 g, 2 × 60 min/d, 2 hr refractory period) however, were able to increase the proliferation of CHO-suspension cells by 210% and T-cells by 20.3%. Importantly, we also reported that T-cell response to LIV was in-part dependent upon AKT phosphorylation, as inhibiting AKT phosphorylation reduced the proliferative effect of LIV by over 60%, suggesting that suspension cells utilize mechanism(s) similar to adherent cells to sense specific LIV signals. Particle image velocimetry combined with finite element modeling showed high transmissibility of these signals across fluids (>90%), and LIV effectively scaled up to T75 flasks. Ultimately, when LIV is tailored to the target cell population, it's highly efficient transmission across media represents a means to non-invasively augment biomanufacturing endpoints for both adherent and suspended cells, and holds immediate applications, ranging from small-scale, patient-specific personalized medicine to large-scale commercial biocentric production challenges.

Keywords

Biomanufacturing; Cell proliferation; Mechanical stimulation; Biomechanics; Adherent cells; Suspension cells; Stem cells; Vibration

1. Introduction

Biomanufacturing depends on the use of living cells cultured in bioreactors.[1] These cells are used to produce living biomaterials and therapeutic biomolecules, as well as to boost host-cell numbers *ex vivo* for personalized medicine. Current and future biomanufacturing applications include, but are not limited to, therapeutic protein production, treatment of cancer,[2] enhancement of the immune system, combating infectious diseases, ameliorating metabolic dysfunction and building bioactive scaffolds for tissue engineering and regeneration.[3-7]

As the demand for biomanufactured products increases, cost-effective optimization strategies are essential to improve yields in large-scale commercial production of therapeutic proteins, or to more quickly expand cell numbers for personalized medicine applications including autologous immunotherapy.[8] Bioreactor systems have become an indispensable element of this biomanufacturing process,[9] fostering a controlled biological, chemical and physical microenvironment to optimize cellular proliferation rate, stem cell differentiation, protein production, and tissue development.[10] Thus, bioreactors are critical for providing not only a standardized, high-quality cell-based product, but for fostering a relevant yield of therapeutic cells.[11,12] However, the complexity of biological systems makes it difficult to design a generic bioreactor capable of controlling cell proliferation and functionality

efficiently and across all cell types, a limitation that contributes to long biomanufacturing periods, disappointing yields and expensive therapies.[13,14]

Traditionally, optimization schemes using *biological* strategies to improve cell yields involve invasive cell line development via vector genetic engineering, cell engineering or omics-based approaches to modulate and ultimately improve the transcriptional activities, and the time integral of viable cell concentration and/or specific productivity.[15,16] From a *chemical* approach, culture media formulation and the chemical environment may be modulated but carries a non-zero risk of jeopardizing sterile culture systems by introducing or refreshing chemical additives, and in some cases necessitates development of complex and costly closed-loop systems. The *physical* domain has also been shown to be important in bioprocessing, with a focus on substrate modulus[17] and topology[18] or dynamic fluid motions,[19] as a means of delivering mechanical cues to adherent cells.[20] Indeed, rocking, rotating and perfusion bioreactor systems that deliver fluid perturbations are commonly available and routinely used to maintain homogeneity across the media in favor of static cultures where cell expansion is comparatively slow. Despite the clear benefit of bioreactors, targeting specific cell types and biological processes via tailored mechanical signals beyond a simple fluid agitation may require specialized technology, with the industry remaining unenthusiastic about processes that require expensive and time-consuming modifications to existing instrumentation and infrastructure.[15,21] Therefore, there is a need to determine if one generic mechanical signal suits this purpose universally across distinct cell types, and if not, define cell-specific signals which promote rapid expansion during the culture phase of cell-based biomanufacturing.[12,22]

Low Intensity Vibration (LIV) is a dynamic mechanical signal characterized as low-magnitude (<1 g peak-to-peak, where g = 9.8 ms^{-2}, Earth's gravitational field) and delivered at a relatively high-frequency (10–500 Hz). If shown effective, utilization of LIV promises a non-invasive, low cost and adaptable technology to augment proliferation rates in multiple cell types and could be readily integrated into existing bioreactor technology of varied design, particularly if the vibration signal transmits uniformly through the fluid. Herein, we explore LIV's potential to promote cellular proliferation in both adherent and suspended cell culture systems. Beyond intensity and frequency, LIV variables include duration, dose number and refractory period (Fig. 1a).

LIV has been shown, *in vivo*, to protect bone quality and promote bone regeneration in mice,[23] rats,[24] turkeys,[25] sheep,[26] and humans.[27] Applied to *in vitro* cell-based studies using adherent cells, LIV has been shown to influence lineage selection,[23,28] and promote expansion of Mesenchymal Stem Cells [MSCs].[29,30] While the mechanisms underlying cell mechanosensitivity to vibration are numerous and complex, it is well known that LIV acts through integrin signaling,[31] including recruitment of Focal Adhesion Kinase (FAK) and AKT to induce RhoA-mediated cell contractility[32,33] as well as activating mechanically sensitive signaling molecules βcatenin[34] and Yes1 Associated Transcriptional Regulator (YAP)[31,35,36] that play interdependent roles in regulating cell proliferation in response to mechanical stimuli.[37-39] These effects have been demonstrated in a wide range of cell types including MSCs, Hematopoietic Stem Cells (HSCs), myoblasts, and skin cells to name a few. Mounting evidence indicates that, as opposed to substrate strains and fluid shear

stress that serve to distort and deform the cell membrane, LIV acts independent of substrate interaction by generating intracellular signals through the Linker of Nucleoskeleton and Cytoskeleton (LINC) complexes of the nuclear envelope by inertial forces generated by oscillatory accelerations.[40] While disabling LINC function is sufficient to mute LIV-induced signaling,[41-43] neither LINC complex,[32] nor the nucleus itself[44] are necessary for activating the signaling events initiated by substrate strain. Consequently, LIV-induced effects on MSCs,[45] osteoblasts[46] and osteocytes[47] are largely independent of the LIV-induced fluid shear stress and substrate strain across multiple frequency/magnitude combinations.

Despite the demonstrated ability of LIV to influence adherent cell culture systems, it is unknown if the LIV signal, and the acceleration/deceleration of the cell, independent of substrate distortion, is applicable to cells grown in suspension. While many mechano-sensing pathways are conserved across cell types, it is entirely possible that suspension cells, such as suspension CHO or T cells, would not respond to LIV, or for that matter, require a mechanical signal distinct from adherent cells. CHO cells were chosen as our cell-type of interest, due to their prevalence in the pharmaceutical and biotech industries, and their ability to be cultured as either adherent or suspension cells.[48] Our study ultimately seeks to determine if LIV represents a non-invasive, non-pharmacological engineering strategy to foster a proliferative response in cell types commonly used in biomanufacturing and autologous cell therapy, such as CHO cells and T cells, without altering functionality or viability.

2. Materials & methods

2.1. Delivery of LIV via a feedback-controlled system

Originally designed for *in vivo* use, low magnitude, high frequency, mechanical signals are delivered using LIV via a closed-loop acceleration feedback-controlled system.[49] For *in vitro* cell culture studies, the LIV system was modified to accommodate cell culture vessels (*e.g.*, microplates and T75 flasks), and be used under sterile cell culture conditions including a high humidity environment within an incubator (Fig. 1a). The LIV device is controlled by an electromagnetic actuator, generating vertical oscillations, while a damped-spring/slider system ensures a smooth sinusoidal signal. The LIV signal is monitored with a plate-mounted accelerometer and controlled through current driving closed-loop error feedback proportional-integral-derivative (PID) controller (*LabVIEW NI*, TX).

To protect from humidity, all electronic components were housed in an airtight plexiglass enclosure, enabling 24/7 automated regulation and monitoring. LIV signals were delivered to cell culture vessels at prescribed magnitudes and frequencies depending on the signal required for each experiment, ranging from 0.1 g to 1.2 g peak-to-peak and 10 Hz–500 Hz, respectively (±5%). Starting parameters for frequency and magnitude for the LIV signals were selected based upon previous data from *in vitro* studies of other adherent cell types such as MSC,[50] pre-osteoblasts and osteocytes.[51] Additional parameters included the number of LIV bouts per day, signal duration per bout, and refractory period (time elapsed between bouts; Fig. 1a).[52]

2.2. Quantifying the transmissibility of LIV signals to suspended cells

In order to determine LIV-induced fluid motions and transmissibility of the signal across culture media in 6-well plates, we used a Finite Element Model (FEM) to derive LIV-induced fluid shear stresses *in vitro* during 0.7 g, 90 Hz vertical vibration (Abaqus 6.9.1, Simula, RI).[46] The culture well was modeled as a deformable shell element (Polystyrene E = 3 GPa). Vertical vibrations were applied as a velocity boundary condition to cylindrical walls while the well bottom was not constrained and was free to deform. As the 6-well plates have an outer rim that extends lower than the bottom of the well plate we did not need to model a connection between the bottom of the well and the top of our vibrating plate. A Eulerian-Lagrangian contact algorithm was used to model fluid motion due to LIV. A conceptual schematic and the analysis region of interest are shown in Fig. 2, highlighting the fact that fluid motion is uniform and that it generally follows the velocity of the fluid container. This figure is representative of the FEM conditions for other variables and previously we have reported that this approach was generalizable for 0.01 g, 0.1 g, 0.5 g 1 g for 30, 50, 70 and 90 Hz signal combinations.[53]

To explore the feasibility of scaling up the overall cell expansion using larger culture vessels, LIV signal transmissibility and fluid motion was also experimentally measured in vertically oscillating T75 vessels (Fig. 3), comparing completely filled flasks to manufacturer suggested partially filled fluid volumes using particle image velocimetry.[46]

Speckles with 1 g/mL density (Cospheric, VIOPMS 63-75um) were suspended for tracking fluid motion. To track light-reflective speckles, a white LED light source was used, and the motion of the surface was captured with a high-speed camera (Photron UX50, San Diego, CA) at a rate of 2000 frames per second (fps). Culture vessels were vibrated vertically at 90 Hz with an acceleration of 0.7 g peak-to-peak, requiring a vertical displacement of approximately 20 μm. Recording of sample motion was started 15 s after the start of LIV to ensure that steady state was reached. Recorded high speed videos at 2000fps were analyzed using previously developed CASI software.[46] For this analysis, we compared the fluid motion differential between t = 0 and t = $\pi/2$ time points that correspond to the peak cycle displacement of 20 μm. This analysis was repeated for 30 Hz and 500 Hz using filled T75 flasks to experimentally quantify the transmissibility of LIV signals to cells cultured in suspension in larger volume conditions.

2.3. CHO-adherent cell culture

CHO-adherent cells were cultured in an incubator at 37 °C and 5% CO_2 (cells were provided by G. Balazsi at Stony Brook University). Prior to the experiment, on day 0, cells were plated in 6-well tissue culture treated plates at the concentration of 6×10^4 cells/ml in 2 ml of supplemented Ham's F–12 K (89% Ham's F–12 K [cat. 21127022], 10% FBS [cat. 16140071], 1% penicillin/streptomycin [cat. 15070063]; *Life Technologies*, NY) per well. Cells were allowed to attach to the surface and grow overnight. Starting 24 hr after plating, cells were either subject to LIV (V; n = 6) or sham-handled (NV; n = 6) for 3 days. Sham handled cells were removed from the incubator and placed on a separate bench top in the same manner as the LIV cells were handled. On day 4, cells were trypsinized (0.05% Trypsin–EDTA [cat. 25300054]; *Life Technologies, NY*) and counted with 1:1 ratio of cell

solution: Trypan Blue (cat. 15250061; *Life Technologies*) to assess cell viability using an automated cell counter (Countess II FL; *Thermo Fisher Scientific*, MA).

2.4. CHO-suspension cell culture

CHO-suspension cells were plated at a concentration of 7.5 × 10^4 cells/mL in Freestyle CHO Expression medium supplemented with 8 mM L-glutamine ([cat. 25030149]; *Thermo Fisher Scientific*, MA) in 125-mL disposable polycarbonate Erlenmeyer flasks with vented caps (*Fisher Scientific*, NH) and cultured in a CO_2 cell incubator at 37 °C and 8% CO_2. Starting 24 hr after plating, cells were either subjected to LIV (V; n = 6) or sham-handled (NV; n = 6) for 3 days. Cells were counted with 1:1 ratio of cell solution: Trypan Blue (*Life Technologies*, NY) using an automated cell counter (Countess II FL; *Thermo Fisher Scientific*, MA).

2.5. T cell culture

Human-derived CD3+ Pan T cells, CD4+ T cells, and CD8+ T cells *(HemaCare*, NY) were obtained from Caucasian male donors. CD3+ cells were isolated using negative selection, and all were cultured in 24-well plates or 6-well plates, with supplemented RPMI (95% RPMI [cat. 11875093], 5% FBS, 1% penicillin/streptomycin; *Life Technologies*, NY) at 37 °C and 5% CO_2. Seeding concentrations for all culture vessels were 0.5×10^6 cells/mL with Dynabead® CD3/CD28 ([cat. 11141D; *Thermo Fisher Scientific*, MA) and recombinant interleukin-2 (rIL-2, [cat. PHC0026,10 ng/mL; *Thermo Fisher Scientific*, MA) for activation. During the initial activation phase, Dynabeads® were at a 1:2 cell:bead ratio. Once a sufficient cell number had been reached to begin experimentation, Dynabeads® were removed using a DynaMag™ (*Thermo Fisher Scientific*, MA) magnet and replenished at a 1:10 cell:bead ratio 24 hr prior to the start of the experiment.

Following plating, T cells were either subjected to LIV (V) or sham-handled (NV). Cell counts were performed every 24 hr prior to receiving LIV doses on representative aliquots. Dynabeads® were removed before mixing the cell suspension with Trypan Blue at a 1:1 ratio of cell solution: Trypan Blue. Counts were taken on each sample using an automated cell counter (Countess II FL; *Thermo Fisher Scientific*, MA). The average of these counts was considered the cell number for the day, and the milestone of proliferation. Cell viability was measured using the flow cytometry stain 7-AAD performed on an LSRFortessa™ (*Becton Dickinson Biosciences*, NJ). Positive and negative gating was determined using isotype controls. Data was analyzed with FlowJo software (Version 10.8.0., Treestar, Ashland, OR, USA). When described, AKT inhibitor VIII ([cat. 124,017]; *Sigma Aldrich, MA*) was added at a concentration of 1uL/mL for the entirety of the culture period.

2.6. Statistical analysis

Experiments were reproduced as independent runs equal to the number of n listed. Each data point in every figure was obtained from a separate reproduction of the experiment. Data normality was assessed with a Shapiro–Wilk test ($\alpha = 0.05$). Depending on the normality of the data, either a Student's t-test or Mann–Whitney U test were performed to measure the mean difference between two groups (*GraphPad Prism*, CA, Ver 9.0.0). A Student's t-test was used in situations where the data were normally distributed, and the

Mann Whitney U test in cases where the dataset was found to be non-normally distributed. In the case of analyzing the mean difference between at least three groups, datasets with a normal distribution were analyzed with a one-way ANOVA (Turkey's post-hoc test), and non-normally distributed data were analyzed using the Kruskal–Wallis test (Dunn's post-hoc test). All tests were performed with $\alpha = 0.05$, a power of 95% with $p < 0.05$ being considered statistically significant.

3. Results

3.1. Transmission of LIV across media to suspended cells

To test the transmissibility of the vibration signal on stacked flasks, single, two or three flask configurations were vibrated at 30 Hz with acceleration magnitudes of 0.2 g and 0.3 g. The vibration magnitude readings at the top of the flask were compared to a reference accelerometer attached to the vibrating platform. Transmissibility, defined as the ratio of reference plate acceleration to flask acceleration was calculated. Our results show that the transmissibility ratio was very close to 1 for each tested condition, showing that 100% of the signal was successfully transferred to stacked flasks. These experiments show that at 30 Hz, at both 0.2 and 0.3 g, the transmissibility function is essentially 1, meaning 100% of the mechanical signal delivered by the device is transmitted to the top flask. This work also demonstrates that LIV can be transmitted effectively at larger scales, setting the groundwork for future scale up experiments.

In 6-well plates, the peak surface strain at $t = \pi/2$ was 1.4με (microstrain). Comparing the peak velocities of both the 6-well wall and the fluid showed a matching velocity of 27 mm/s (Fig. 2a). Further, fluid velocity showed no large gradients across the well height indicating that the attached and suspended cells experience lossless LIV transmittance from the actuator. While the lossless transmission of LIV in 6-well plate is largely due to small plate deformations due to well-supported and small surface area (~10 cm^2), T75 flasks have considerably larger surface (75 cm^2) and result in larger effective deformations during LIV. As reported by our group[32] and others,[54,55] bending motions in a vertically oscillating elastic culture plate will result in fluid motions that will propagate to the fluid surface thus altering the acceleratory motions experienced by suspended cells. A common strategy to limit fluid motions is to fill the culture vessel to minimize differential accelerations between gas and liquid mediums.[35] Therefore, to test whether filling a culture vessel maximizes the transmittance of vertical accelerations to fluid we quantified the acceleration transmittance in fluid-filled, vertically-oscillating culture vessels and compared it to manufacturer suggested fluid volumes (Fig. 2b).

Transmittance was compared from the side view (X-Z plane) while the fluid motion at the surface was compared from the top view (X–Y plane). Side motion of the full flasks is shown in Fig. 3c, fluid motion vectors were parallel to each other and to the actuator motion with a maximum magnitude of 18 μm, essentially matching to the 20 μm peak motion of the actuator, indicating that fluid particles were vibrating at the same frequency and acceleration magnitude as the actuator. Shown in Fig. 3d, fluid sloshing measured from top view was minimal around 2 μm, again indicating minimal fluid motion in filled flasks. Measuring fluid motions at the fluid/flask boundary in partially filled flasks, we

have observed that fluid was forming standing wave patterns and showed vertical motions across the measured area (Fig. 3e). Fluid displacements during half cycle (0.05 s) reached up to 250 μm, indicating fluid towards the surface was moving approximately 10 times more than fluid filled flasks. Similarly, fluid movement measured from top view showed motions peaking at approximately 2.5 mm with the fluid surface in a standing wave pattern (Fig. 3f), suggesting that mechanical signals generated by LIV are a product of both acceleration and fluid motion, and each need be considered when calculating acceleration transmittance. LIV Transmissibility of the LIV signal across fluid in filled flasks at 0.7 g acceleration exceeded 95%, and was highly similar between signals operating at 30, 90 & 500 Hz (n = 3; Fig. 3g), suggesting that LIV-induced harmonic motions of the flask surface were directly transmitted to the fluid with minimal loss across wide ranges of frequencies.

3.2. Proliferative LIV signal for adherent cells hampers growth for suspension cells

To minimize potential differences between our representative adherent and suspension cells we compared CHO cells grown as adherent cells to those grown as suspension culture conditions. We first tested the effect of a LIV regimen with multiple refractory periods, first optimized for use with MSCs,[56] on adherent CHO cells. Control and experimental cells were plated on Day 0 and allowed to adhere to the plate overnight. 24 hr after plating, adherent-CHO cells were subjected to a LIV signal for 3 days that was delivered at 0.2 g and 500 Hz in 3 × 30 min/d doses with a 2 hr refractory period between each dose. At day 4, cells were counted, and cell numbers were compared against a sham LIV control. Following 96 h, CHO adherent cells subjected to the LIV program showed a 79 ± 30.7% increase in cell number compared to sham controls ($n = 6$, $p < 0.05$; Fig. 4a).

We delivered the same LIV signal parameters to CHO-suspension cells. Plated on Day 0 and allowed to grow overnight, LIV cells were then subjected to the identical signal as the CHO-adherent cells (0.2 g, 500 Hz, 3 × 30 min/d doses, 2hr refractory period), and compared to sham LIV suspension controls. At day 4, LIV-treated CHO-suspension cell population had fallen −13 ± 10.1% below sham LIV controls ($n = 6$, $p < 0.05$; Fig. 4b). While these data confirm that CHO-suspension cells are mechanosensitive, they also suggest that LIV signal parameters are cell-type specific, and that the same set of parameters that enhance proliferation in adherent cells hampers proliferation in suspension cells.

3.3. LIV signal optimization for suspension cells

To determine whether a LIV signal could be designed to enhance proliferation of suspension cells, a series of experiments were conducted to examine both frequency and intensity of the LIV signal. To determine the optimal frequency for enhancing proliferation, 5 sets of CHO-suspension cells were plated and allowed to culture overnight. Each set of CHO-suspension cells was subjected to a LIV signal with a consistent amplitude of 0.2 g, while the frequency was varied between 0 Hz (sham-LIV control), 30 Hz, 60 Hz, 90 Hz, and 250 Hz between groups. Following 3 days exposure to LIV, cell counts were taken from each group. The 30 Hz frequency increased CHO-suspension cell number by 61 ± 10.1% relative to sham LIV control, while no other frequency showed significant difference to the control ($n = 6$, $p < 0.05$; Fig. 5a).

To determine which LIV intensity would promote the largest increase in CHO-suspension cell proliferation, 5 sets of CHO-suspension cells were plated and allowed to culture overnight. Each set of CHO-suspension cells was then subjected to a LIV signal using the 'optimized' frequency of 30 Hz, with acceleration adjusted to include 0 g (sham-LIV control), 0.35 g, 0.7 g, 1.0 g, and 1.35 g. After 3 days of LIV, cell counts were taken from each group. An acceleration of 0.7 g generated the largest increase in proliferation of 15 ± 6.8% when compared to sham controls ($n = 6$, $p < 0.05$; Fig. 5b), while no other accelerations resulted in a significant difference relative to control. Taken together these data suggest that LIV can enhance proliferation in CHO-suspension cells, but that signal parameters are different than those that increase proliferation in CHO-adherent cells.

3.4. Multiple bouts per day further enhances proliferation of CHO suspension cells

Using CHO-adherent cells, we have previously reported that two LIV bouts separated by a rest period of at least 1 hr was more effective at enhancing proliferation than a single bout of equal total duration.[52] Here we combined the previous optimization of frequency and intensity with a 2 bout per day dosing schedule that was shown to improve LIV efficacy in adherent cells, to determine if CHO-suspension cells benefited multiple bouts per day. CHO-suspension cells were plated and allowed to culture for 24 hr, with one group exposed to LIV (0.7 g, 30 Hz, 2 × 1hr bout/day, 2hr refractory period) for 48 hr, after which cell counts were taken. LIV exposed cells showed a 210 ± 34.2% increase in proliferation when compared to sham-LIV controls ($n = 5$, $p < 0.05$; Fig. 6). These data showed that more than a single bout of LIV each day, separated by a 2 hr refractory period, can enhance proliferation of CHO suspension cells, just as it had been shown to do in adherent cells.

3.5. LIV optimization for T cells

To determine if other types of suspension cells would respond to similar LIV parameters, a series of experiments were designed to examine if LIV could enhance T cell proliferation. Like the first optimization experiments done in CHO-suspension cells, 4 groups of T cells were subject to LIV of varying frequencies, including 0 Hz (sham-handled control), 10 Hz, 30 Hz, and 90 Hz, all at an intensity of 0.7 g. After 48 hr of LIV, cells exposed to 30 Hz signal had the greatest increase in proliferation of 24.8 ± 7.8% relative to controls ($n = 5$, $p < 0.05$; Fig. 7a). Next, examining signal intensity, 4 groups of T cells were subject to LIV to include 0 g (control), 0.1 g, 0.7 g, and 1.2 g, each delivered at the 'optimized' frequency of 30 Hz. Following 48 hr of treatment with the LIV protocol, cells exposed to a 0.7 g acceleration had the most significant proliferative response with 20.3 ± 7.6% greater than controls. ($n = 6$, $p < 0.02$). Finally, examining bouts per day, experiments were designed to determine if repeated dosing with 'optimized' LIV frequency and acceleration resulted in an effect on T cell proliferation. T cells were separated into 4 groups: controls, 1 bout of LIV/day, 2 bouts/day, and 3 bouts/per day, with each bout separated by a 2 hr rest period. We observed that both 2 and 3 bouts of LIV enhanced proliferation significantly, with the 2 bouts enhancing proliferation by 22.7 ± 14.4% as compared to controls, and three bouts per day enhancing proliferation by 29.4 ± 4.3% as compared to controls ($n = 6$, $p < 0.05$; Fig. 7b). Though the 3 bouts per day condition enhanced proliferation the most over control, there was no significant difference between the 2 and 3 bout conditions.

The impact of LIV on general cell health was examined using the cell viability marker 7AAD. Human primary T cells were cultured for 5 d in T 25 flasks, with one group exposed to LIV (0.7 g, 30 Hz, 2 × 1 hr bout/day, 2 hr refractory period). Flow cytometry was performed on day 5 to analyze incorporation of 7AAD. LIV expanded cells showed no significant changes in cell viability (4.5% increase ± 20.1% in 7AAD staining, $p > 0.5$, $n = 6$). Ultimately, these data suggest that LIV signal parameters, including frequency, amplitude, and number of bouts per day, can be tailored to drive a significant increase in T cell proliferation without any negative effects on cell viability.

3.6. Inhibition of AKT reduces proliferative effect of LIV on T cells

LIV phosphorylates of AKT on Ser 473 residue in adherent MSCs, leading to activation βcatenin[56] and it's nuclear accumulation,[34] where βcatenin depletion leads to decreased proliferation.[37] In order to begin to elucidate the mechanism behind LIV's effect on T cells in suspension we determined whether LIV's effect on T cell proliferation was affected by AKT phosphorylation. T-cells were subjected to LIV (30 Hz, 0.7 g, 2 × 60 min/d, 2 hr refractory period, n = 6/group) for five days with or without an AKT inhibitor VIII [AKTi] (Selleckchem, 1uL/mL). Every 24 h, cell numbers were evaluated and inter-group differences were evaluated. During 5 days AKTi addition (AKTi+) did not affect cell proliferation in non-LIV groups. In cells without the AKTi treatment (AKTi−), LIV increased the T-cell proliferation by 12.9% ($p < 0.05$), 21.6% ($p < 0.01$) and 24.9% ($p < 0.01$) at days 3, 4, and 5, respectively. On days 3 and 4, cell numbers of AKTi+ control and LIV groups were not different from each other and when compared to AKTi− controls. At day 5, LIV treated AKTi+ cells only grew 9.3% more than their AKTi+ controls ($n = 6$, $p < 0.05$; Fig. 8) which was a 62% decrease compared to LIV effect in AKTi groups. This suggests that LIV's effect on T cells is controlled, at least in part, through activation of AKT.

4. Discussion

Mechanical stimulation represents a relatively underutilized strategy for enhancing biomanufacturing outcomes. Our studies show that physical signals, delivered in the form of Low Intensity Vibration (LIV), can augment proliferation in both adherent and suspension cell types, but that the LIV signal is cell-type specific, with each cell-type responding differently to distinct signal configurations. Our finding that the LIV signal can be tailored to enhance expansion of both adherent and suspension cells is encouraging and suggests that LIV could be used to improve many different existing biomanufacturing processes once the influential parameters are identified.

LIV was initially developed to mimic the power spectrum of muscle contractility during exercise, as a surrogate for functional load bearing.[57] There is a wealth of literature describing the beneficial effects of exercise on a number of adherent and suspension cells within the body,[27] including immune cells.[58] Previous work from our lab has demonstrated that LIV can markedly influence lineage selection in MSCs *in vivo*,[23] an effect that can be translated to *in vitro* applications.[52] What was not clear was if cells in suspension – insulated from substrate strain – were also sensitive to the accelerations/decelerations of LIV, and if so, what the signal parameters would be that would drive the response. By their

very definition, adherent cells are anchored to substrates via several adhesion molecules that are associated with the cytoskeleton. Since suspension cells lack this tethering, they likely perceive physical perturbations such as matrix strains and fluid shearing in a different way than adherent cells. A principal finding of the work presented here is that LIV is efficiently transmitted (>90% transmissibility) across fluids to cells in suspension, whether 24-well, 6-well plates or fully-filled T75 flasks. Additionally, LIV was efficiently transmitted to multiple stacked flasks, with no loss of magnitude with three flasks stacked one on top of the other. The only exception to this finding was the partially-filled T75 flasks where fluid movement added significantly to the LIV motions caused by the vertically oscillating elastic flask-bottom.[54,55] Therefore no experiments were conducted with partially-filled T75 flasks. Fully filled flasks are commonly used in microgravity studies to limit fluid motion, and we have previously reported that cells are able to grow within fully filled flasks for up to 72 h.[35,43] The use of fully filled flasks does represent a challenge to the clinical utility of this work, as nearly all cell culture in basic science research and commercial manufacturing utilize partially filled containers, to allow for gas exchange. If the use fully filled flasks are required to ensure the uniformity of fluid motion, then one would consider implementing some sort of closed loop fluid exchange system to ensure adequate oxygenation and nutrient transport to the cells in culture.

When conducting experiments with CHO cells, we opted to use Erlenmeyer flasks with a substantially well supported and stiff bottom to limit wall deformations. The fact that both CHO cells and T-cells favored 30 Hz response suggests that and that acceleration itself as the driving factor. These findings further indicate that if structural response of the culturing vessel is well controlled, consistently transmitting LIV to adherent and suspended cells in a scalable way is possible. While the data reported here demonstrate that both adherent and suspended cells can respond to LIV, the outcome is highly dependent on the signal configuration, including intensity (i.e., magnitude of acceleration), frequency, bout duration, number of bouts per day and the length and number of refractory period(s). Importantly, a LIV signal tuned to stimulate expansion in one cell type is distinct from those parameters which drive another cell's response, and thus a bioreactor using LIV to promote expansion would first have to determine the idealized signal parameters to promote a response for that given cell. Further, that suspension cells respond to LIV at all suggests that sensitivity to mechanical signals is not caused by a feature exclusive to adherent cells, or that the way they perceive mechanical signals is distinct from each other. Cells are as much an accelerometer as they are a strain gage. There are, of course, an infinite number of signal parameter combinations, and we readily recognize some may prove to yield a more robust proliferative response, or an idealized set of parameters for one type of cell (or cell density) may work distinctly different for another set. However, this work demonstrates both that suspension cells are capable of sensing and responding to mechanical signals (cell as an accelerometer rather than strain gage) and that adherent and suspension cells are tuned to different mechanical parameters. Further work is needed to fully optimize signal parameters for suspension cells, and indeed for different suspension cell types, as this work demonstrates that mechanosensation is highly cell-type specific.

Cell density also plays an important role in the expansion of both adherent and suspension cells, but this is a variable that is beyond the scope of this paper. While CHO cells are

generally grown at high cell densities, overcrowding will hamper growth due to a number of factors including contact inhibition or changes in media acidity and nutrients. In all cases we maintained cell cultures at densities that have been studied in prior literature, are not considered ‘too dense’, and are used in the biomanufacturing industry.[59,60]

One possible explanation for why suspension cells require signal parameters distinct from adherent cells could be a difference in the transmissibility of LIV. Undoubtedly, the way distortion/distention of the bottom of a flask is perceived by an adherent cell is different than how acceleration is perceived by a suspension cell. Indeed, suspension cells required a signal with a much higher amplitude (0.7 g as compared to 0.2 g for adherent cells) which suggests that the initial signal needs to be higher in magnitude for the suspension cells to “perceive” the same acceleration as the adherent cells. Importantly, a mechanical signal driven at a lower frequency will maintain its amplitude over longer distances and through less transmissible substrates. A signal with a higher frequency – and thus a much smaller displacement for a given acceleration - will attenuate much more quickly than a lower frequency signal.

Differences in stiffness of adherent versus suspension cell might account for their distinct responses to LIV.[61] Given that the cytoskeleton contributes greatly to the biomechanical properties *(e.g.*, stiffness) of a cell,[18] it is plausible that a “softer” cell may respond differently to LIV than a “stiffer” cell. AFM studies have provided direct evidence that mechanical connections between extracellular matrix proteins and the actin cytoskeleton indeed exist.[62] The differential stiffness of adherent and suspension cells is, in part, due to their physical attachment, or lack thereof, to a surface. In attached cells, stiffness increases with development of actin fibers within a cell. Additionally, more focal adhesion complex (FAC) clusters are formed in cells attached to 3D suspended structure compared to cells attached to a 2D flat surface. The enhanced formation of focal adhesions may account for the enhanced susceptibility of adherent cells to LIV. Less efficient transmission of vibration to the nucleus might also help explain why a higher intensity was required for suspension cells to “sense” the same vibration, and suggests that conditions that disrupt the cell cytoskeleton, such as aging, will compromise mechanosensitivity.

Interestingly, previous data has confirmed that in adherent cells, a single bout of LIV will transiently induce cell-wide cytoskeletal remodeling and enhanced formation of focal adhesion clusters.[63] This cytoskeletal remodeling essentially “primes” a cell by improving coupling of the nucleus to the plasma edge of the cytoskeleton and increases overall sensitivity to subsequent mechanical signals. That suspension cells also benefitted from repeated dosing with LIV, suggests that mechano-sensation in suspension cells might involve a similar type of cytoskeletal remodeling shown to play a role in adherent cells, and with enhanced cytoskeletal architecture, a ratcheted-up response to follow-on mechanical input.

Focusing on the T cell response, the work reported here shows that LIV can enhance T cell proliferation. When considered in the context of published work that reports that whole body vibration can elicit an immune response,[64,65] it may help translate these low intensity signals to a safe clinical application for LIV as a method to enhance immune function. It is well established that the mechanical environment plays a critical role in T cell activation

and proliferation.[66] The T cell receptor [TCR] has been classified as a mechanoreceptor and transduction of mechanical signals from the TCR is involved in modulating T cell recognition, signaling, metabolism, and gene expression.[67] Upon binding to an antigen and formation of an immunological synapse T cells also undergo dynamic reconfiguration of their cytoskeleton to better allow for precise mechanotransduction. The results reported here indicate that T cells are directly responsive to LIV and may represent a unique method for promoting T cell expansion. Additionally, it is of note that two very different types of suspension cells (CHO-suspension cells and T cells) were independently found to respond to the same set of signal parameters. This gives some support to the notion that the alteration of signal parameters between adherent and suspension cells was due to changes in transmission of the acceleration signal (i.e. altering signal parameters to generate the same changes in acceleration at the cell nucleus), and not a fundamental difference between adherent and suspension cell cytoskeletal architecture or inherent mechanosensitivity.

We found that inhibition of AKT reduced the proliferative effect of LIV on T cells by over 60%. This suggests that LIV's effect on T cell proliferation is mediated, at least in part, by enhanced activation of the AKT signaling pathway. Prior research on the effects of mechanical stimulation in MSCs confirms that mechanical vibration, like LIV, can non-invasively phosphorylate (and activate) the protein AKT.[68,69] It is well known that mechanosensitive proteins, like AKT, are highly conserved across cell types.[70] In T cells, AKT is part of central activation pathways that govern T cell proliferation and functionality.[71,72] This, coupled with our evidence showing that inhibition of AKT reduces the effect of LIV on T cell proliferation, suggests that LIV acts directly on mechanosensitive proteins like AKT in multiple cell types. Importantly, inhibition of AKT did not eliminate LIV's effect on the T cells, suggesting that LIV acts to improve T cell proliferation through numerous mechanisms, of which AKT is just one part. However, this initial exploration of the mechanism of action for LIV in T cells suggests that LIV would have significant effects on T cell functionality as well, since the AKT signaling pathway is directly linked to T cell activation and effector function.

It is important to note that for all experiments reported here that cell proliferation was estimated by reporting daily cell counts. While we have conducted a basic study of the effect of LIV on cell viability and apoptosis, a more accurate analysis of changes in proliferation versus apoptosis via trypan exclusion may be warranted in addition to assessment of daily cell number. Further studies will also need to be done to determine to what effects LIV has on cell viability and functionality if this strategy should be considered for more complex biomanufacturing workflows like autologous cell therapy.

In summary, we have shown that LIV can significantly enhance proliferation of both adherent and suspended CHO cells, *in vitro*, which may translate to both biomanufacturing and autologous cell therapy industries. Our results have demonstrated that the LIV configuration is cell-type specific, meaning that what promotes proliferation in one cell type can hamper it in another. Importantly though, we have demonstrated that the LIV signal is readily ‘tunable,’ and can enhance proliferation in both adherent and suspension cells. Matrix strain and fluid shear are undoubtedly large parts of the mechanical milieu encompassing adherent cells. However, these results emphasize that suspension cells

can benefit from LIV stimulation in the absence of cell anchorage, and suggests that acceleration, and not some property specific to matrix distortion of the cell, is the key driver the LIV's effect on cell proliferation. And certainly, while the biotechnology industry has advanced bioreactors using chemical and biological approaches, there remains room for improvement. The high transmissibility of the LIV signal suggests that it can readily – and non-invasively - be incorporated into existing bioreactor infrastructure, without requiring exposing culture systems to outside agents.

Acknowledgements

We thank Jonathan Wadsworth on his expertise on accelerometer measurements. This work was supported by the Long Island Bioscience Hub funded through the NIH-Research Evaluation and Commercialization Hub (U-HL127522), the Research Foundation Technology Accelerator Fund, the Center for Biotechnology (NYSTAR) as well as grants from NIH (AG059923, P20GM109095) and NSF (1929188 & 2025505).

References

1. Walsh G. Biopharmaceutical benchmarks 2010. Nat Biotechnol. 2010;28(9):917–924. 10.1038/nbt0910-917. [PubMed: 20829826]
2. Schuster SJ, Svoboda J, Chong EA, et al. Chimeric antigen receptor T cells in refractory B-cell lymphomas. N Engl J Med. 2017;377(26):2545–2554. 10.1056/NEJMoa1708566. [PubMed: 29226764]
3. Lutolf MP, Hubbell JA. Synthetic biomaterials as instructive extracellular microenvironments for morphogenesis in tissue engineering. Nat Biotechnol. 2005;23(1):47–55. 10.1038/nbt1055. [PubMed: 15637621]
4. Nakashima M, Reddi AH. The application of bone morphogenetic proteins to dental tissue engineering. Nat Biotechnol. 2003;21(9):1025–1032. 10.1038/nbt864. [PubMed: 12949568]
5. Oberpenning F, Meng J, Yoo JJ, Atala A. De novo reconstitution of a functional mammalian urinary bladder by tissue engineering. Nat Biotechnol. 1999;17(2):149–155. 10.1038/6146. [PubMed: 10052350]
6. Reddi AH. Role of morphogenetic proteins in skeletal tissue engineering and regeneration. Nat Biotechnol. 1998;16(3):247–252. 10.1038/nbt0398-247. [PubMed: 9528003]
7. Shea LD, Smiley E, Bonadio J, Mooney DJ. DNA delivery from polymer matrices for tissue engineering. Nat Biotechnol. 1999;17(6):551–554. 10.1038/9853. [PubMed: 10385318]
8. Shah NN, Fry TJ. Mechanisms of resistance to CAR T cell therapy. Nat Rev Clin Oncol. 2019;16(6):372–385. 10.1038/s41571-019-0184-6. [PubMed: 30837712]
9. Stephenson M, Grayson W. Recent advances in bioreactors for cell-based therapies. F1000Research. 2018;7. 10.12688/f1000research.12533.1.
10. Polak JM, Mantalaris S. Stem cells bioprocessing: an important milestone to move regenerative medicine research into the clinical arena. Pediatr Res. 2008;63(5):461–466. 10.1203/PDR.0b013e31816a8c1c. [PubMed: 18427288]
11. Eaker S, Abraham E, Allickson J, et al. Bioreactors for cell therapies: current status and future advances. Cytotherapy. 2016;19. 10.1016/j.jcyt.2016.09.011.
12. Garcia-Aponte OF, Herwig C, Kozma B. Lymphocyte expansion in bioreactors: upgrading adoptive cell therapy. J Biol Eng. 2021;15(1):13. 10.1186/s13036-021-00264-7. [PubMed: 33849630]
13. Salehi-Nik N, Amoabediny G, Pouran B, et al. Engineering parameters in bioreactor's design: a critical aspect in tissue engineering. BioMed Res Int. 2013;2013:762132. 10.1155/2013/762132. [PubMed: 24000327]
14. Saini KS, Svane IM, Juan M, Barlesi F, André F. Manufacture of adoptive cell therapies at academic cancer centers: scientific, safety and regulatory challenges. Ann Oncol. 2021;33(1):6–12. 10.1016/j.annonc.2021.09.020. [PubMed: 34655734]

15. Kim JY, Kim YG, Lee GM. CHO cells in biotechnology for production of recombinant proteins: current state and further potential. Appl Microbiol Biotechnol. 2012;93(3):917–930. 10.1007/s00253-011-3758-5. [PubMed: 22159888]
16. Gupta P, Lee KH. Genomics and proteomics in process development: opportunities and challenges. Trends Biotechnol. 2007;25(7):324–330. 10.1016/j.tibtech.2007.04.005. [PubMed: 17475353]
17. Özkale B, Sakar MS, Mooney DJ. Active biomaterials for mechanobiology. Biomaterials. 2021;267:120497. 10.1016/j.biomaterials.2020.120497. [PubMed: 33129187]
18. Discher DE, Janmey P, Wang YL. Tissue cells feel and respond to the stiffness of their substrate. Science. 2005;310(5751):1139–1143. 10.1126/science.1116995. [PubMed: 16293750]
19. Banes AJ, Horesovsky G, Larson C, et al. Mechanical load stimulates expression of novel genes in vivo and in vitro in avian flexor tendon cells. Osteoarthritis Cartilage. 1999;7(1):141–153. [PubMed: 10367022]
20. Ingber DE. Tensegrity and mechanotransduction. J Bodyw Mov Ther. 2008;12(3):198–200. 10.1016/j.jbmt.2008.04.038. [PubMed: 19083675]
21. Stolfa G, Smonskey MT, Boniface R, et al. CHO-omics review: the impact of current and emerging Technologies on Chinese hamster ovary based bioproduction. Biotechnol J. 2018;13(3):e1700227. 10.1002/biot.201700227. [PubMed: 29072373]
22. Li F, Vijayasankaran N, Shen AY, Kiss R, Amanullah A. Cell culture processes for monoclonal antibody production. mAbs. 2010;2(5):466–479. 10.4161/mabs.2.5.12720. [PubMed: 20622510]
23. Rubin CT, Capilla E, Luu YK, et al. Adipogenesis is inhibited by brief, daily exposure to high-frequency, extremely low-magnitude mechanical signals. Proc Natl Acad Sci USA. 2007;104(45):17879–17884. [PubMed: 17959771]
24. Rubin C, Xu G, Judex S. The anabolic activity of bone tissue, suppressed by disuse, is normalized by brief exposure to extremely low-magnitude mechanical stimuli. FASEB J. 2001;15(12):2225–2229. 10.1096/fj.01-0166com. [PubMed: 11641249]
25. Qin YX, Rubin CT, McLeod KJ. Nonlinear dependence of loading intensity and cycle number in the maintenance of bone mass and morphology. J Orthop Res. 1998;16(4):482–489. 10.1002/jor.1100160414. [PubMed: 9747791]
26. Rubin C, Turner AS, Bain S, Mallinckrodt C, McLeod K. Anabolism. Low mechanical signals strengthen long bones. Nature. 2001;412(6847):603–604. 10.1038/35088122.
27. Pagnotti GM, Styner M, Uzer G, et al. Combating osteoporosis and obesity with exercise: leveraging cell mechanosensitivity. Nat Rev Endocrinol. 2019;15(6):339–355. 10.1038/s41574-019-0170-1. [PubMed: 30814687]
28. Bas G, Loisate S, Hudon SF, et al. Low intensity vibrations augment mesenchymal stem cell proliferation and differentiation capacity during in vitro expansion. Sci Rep. 2020;10(1):9369. 10.1038/s41598-020-66055-0. [PubMed: 32523117]
29. Frechette DM, Krishnamoorthy D, Pamon T, Chan ME, Patel V, Rubin CT. Mechanical signals protect stem cell lineage selection, preserving the bone and muscle phenotypes in obesity. Ann N Y Acad Sci. 2017;1409(1):33–50. 10.1111/nyas.13442. [PubMed: 28891202]
30. Chan ME, Uzer G, Rubin CT. The potential benefits and inherent risks of vibration as a non-drug therapy for the prevention and treatment of osteoporosis. Curr Osteoporos Rep. 2013;11(1):36–44. 10.1007/s11914-012-0132-1. [PubMed: 23371467]
31. Goelzer M, Thompson WR, Uzer G. Chapter 2.1 - cells as functional load sensors and drivers of adaptation. In: Niebur GL, ed. Mechanobiology. Elsevier; 2020:79–98.
32. Uzer G, Thompson WR, Sen B, et al. Cell mechanosensitivity to extremely low-magnitude signals is enabled by a LINCed nucleus. Stem Cells. 2015;33(6):2063–2076. 10.1002/stem.2004. [PubMed: 25787126]
33. Thompson WR, Guilluy C, Xie Z, et al. Mechanically activated fyn utilizes mTORC2 to regulate RhoA and adipogenesis in mesenchymal stem cells. Stem Cells. 2013;31(11):2528–2537. 10.1002/stem.1476. [PubMed: 23836527]
34. Uzer G, Bas G, Sen B, et al. Sun-mediated mechanical LINC between nucleus and cytoskeleton regulates betacatenin nuclear access. J Biomech. 2018;74:32–40. 10.1016/j.jbiomech.2018.04.013. [PubMed: 29691054]

35. Thompson M, Woods K, Newberg J, Oxford JT, Uzer G. Low-intensity vibration restores nuclear YAP levels and acute YAP nuclear shuttling in mesenchymal stem cells subjected to simulated microgravity. NPJ Microgravity. 2020;6(1):35. 10.1038/s41526-020-00125-5. [PubMed: 33298964]
36. Lin CY, Song X, Ke Y, et al. Yoda 1 enhanced low-magnitude high-frequency vibration on osteocytes in regulation of MDA-MB-231 breast cancer cell migration. Cancers. 2022;14(14). 10.3390/cancers14143395.
37. Sen B, Paradise CR, Xie Z, et al. β-Catenin preserves the stem state of murine bone marrow stromal cells through activation of EZH2. J Bone Miner Res. 2020;35(6): 1149–1162. 10.1002/jbmr.3975. [PubMed: 32022326]
38. Zhao B, Ye X, Yu J, et al. TEAD mediates YAP-dependent gene induction and growth control. Genes Dev. 2008;22(14):1962–1971. 10.1101/gad.1664408. [PubMed: 18579750]
39. Benham-Pyle BW, Pruitt BL, Nelson WJ. Cell adhesion. Mechanical strain induces E-cadherin-dependent Yap 1 and beta-catenin activation to drive cell cycle entry. Science. 2015;348(6238):1024–1027. 10.1126/science.aaa4559. [PubMed: 26023140]
40. Birks S, Uzer G. At the nuclear envelope of bone mechanobiology. Bone. 2021;151:116023. 10.1016/j.bone.2021.116023. [PubMed: 34051417]
41. Newberg J, Schimpf J, Woods K, Loisate S, Davis PH, Uzer G. Isolated nuclei stiffen in response to low intensity vibration. J Biomech. 2020 October 09;111:110012. 10.1016/j.jbiomech.2020.110012. [PubMed: 32932075]
42. Yi X, Wright LE, Pagnotti GM, et al. Mechanical suppression of breast cancer cell invasion and paracrine signaling to osteoclasts requires nucleo-cytoskeletal connectivity. Bone research. 2020;8(1):40. 10.1038/s41413-020-00111-3. [PubMed: 33298883]
43. Touchstone H, Bryd R, Loisate S, et al. Recovery of stem cell proliferation by low intensity vibration under simulated microgravity requires intact LINC complex. NPJ Micrograv. 2019;5(11). 10.1038/s41526-019-0072-5.
44. Graham DM, Andersen T, Sharek L, et al. Enucleated cells reveal differential roles of the nucleus in cell migration, polarity, and mechanotransduction. J Cell Biol. 2018; 217(3):895–914. 10.1083/jcb.201706097. [PubMed: 29351995]
45. Uzer G, Pongkitwitoon S, Ete Chan M, Judex S. Vibration induced osteogenic commitment of mesenchymal stem cells is enhanced by cytoskeletal remodeling but not fluid shear. J Biomech. 2013;46(13):2296–2302. 10.1016/j.jbiomech.2013.06.008. [PubMed: 23870506]
46. Uzer G, Manske S, Chan M, et al. Separating fluid shear stress from acceleration during vibrations in vitro: identification of mechanical signals modulating the cellular response. Cell Mol Bioeng. 2012;5(3):266–276. 10.1007/s12195-012-0231-1. [PubMed: 23074384]
47. Uzer G, Pongkitwitoon S, Ian C, et al. Gap junctional communication in osteocytes is amplified by low intensity vibrations in vitro. PLoS ONE. 2014;9(3):e90840. 10.1371/journal.pone.0090840. [PubMed: 24614887]
48. Baker KJ, Brown TD, Brand RA. A finite-element analysis of the effects of intertrochanteric osteotomy on stresses in femoral head osteonecrosis. Clin Orthop. 1989;249:183–198.
49. Rubin C, Recker R, Cullen D, Ryaby J, McCabe J, McLeod K. Prevention of postmenopausal bone loss by a low-magnitude, high-frequency mechanical stimuli: a clinical trial assessing compliance, efficacy, and safety. J Bone Miner Res. 2004;19(3):343–351. 10.1359/jbmr.0301251. [PubMed: 15040821]
50. Uzer G, Rubin CT, Rubin J. Cell mechanosensitivity is enabled by the LINC nuclear complex. Curr Mol Biol Rep. 2016;2(1):36–47. 10.1007/s40610-016-0032-8. [PubMed: 27326387]
51. Yi X, Wright LE, Pagnotti GM, et al. Mechanical suppression of breast cancer cell invasion and paracrine signaling to osteoclasts requires nucleo-cytoskeletal connectivity. Bone Res. 2020;8(1):40. 10.1038/s41413-020-00111-3. [PubMed: 33298883]
52. Sen B, Xie Z, Case N, Styner M, Rubin CT, Rubin J. Mechanical signal influence on mesenchymal stem cell fate is enhanced by incorporation of refractory periods into the loading regimen. J Biomech. 2011;44(4):593–599. 10.1016/j.jbiomech.2010.11.022. [PubMed: 21130997]

53. Uzer G, Manske SL, Chan ME, et al. Separating fluid shear stress from acceleration during vibrations in vitro: identification of mechanical signals modulating the cellular response. Cell Mol Bioeng. 2012;5(3):266–276. 10.1007/s12195-012-0231-1. [PubMed: 23074384]
54. Dareing DW, Yi D, Thundat T. Vibration response of microcantilevers bounded by a confined fluid. Ultramicroscopy. 2007;107(10–11):1105–1110. 10.1016/j.ultramic.2007.02.048. [PubMed: 17574760]
55. Cox EA, Gleeson JP, Mortell MP. Nonlinear sloshing and passage through resonance in a shallow water tank. Z Angew Math Phys. 2005;56(4):645–680. 10.1007/s00033-004-3125-9.
56. Sen B, Xie Z, Case N, Styner M, Rubin CT, Rubin J. Mechanical signal influence on mesenchymal stem cell fate is enhanced by incorporation of refractory periods into the loading regimen. J Biomech. 2011;44(4):593–599. 10.1016/j.jbiomech.2010.11.022. [PubMed: 21130997]
57. Huang Robert P, Rubin CT, McLeod KJ. Changes in postural muscle dynamics as a function of age. Journals Gerontology Ser A Biological Sciences and Medical Sciences. 1999;54(8):B352–B357. 10.1093/gerona/54.8.B352.
58. Yoon KJ, Ahn A, Park SH, et al. Exercise reduces metabolic burden while altering the immune system in aged mice. Aging. 2021;13(1):1294–1313. 10.18632/aging.202312. [PubMed: 33406502]
59. Donaldson JS, Dale MP, Rosser SJ. Decoupling growth and protein production in CHO cells: a targeted approach. Front Bioeng Biotechnol. 2021;9:658325. 10.3389/fbioe.2021.658325. [PubMed: 34150726]
60. Xu WJ, Lin Y, Mi CL, Pang JY, Wang TY. Progress in fed-batch culture for recombinant protein production in CHO cells. Appl Microbiol Biotechnol. 2023;107(4):1063–1075. 10.1007/s00253-022-12342-x. [PubMed: 36648523]
61. Maloney JM, Nikova D, Lautenschläger F, et al. Mesenchymal stem cell mechanics from the attached to the suspended state. Biophys J. 2010;99(8):2479–2487. 10.1016/j.bpj.2010.08.052. [PubMed: 20959088]
62. Wang K, Qin Y, Chen Y. In situ AFM detection of the stiffness of the in situ exposed cell nucleus. Biochimica biophysica acta Mol Cell Res. 2021;1868(5):118985. 10.1016/j.bbamcr.2021.118985.
63. Sen B, Guilluy C, Xie Z, et al. Mechanically induced focal adhesion assembly amplifies anti-adipogenic pathways in mesenchymal stem cells. Stem Cells. 2011;29(11):1829–1836. 10.1002/stem.732. [PubMed: 21898699]
64. Song N, Liu X, Feng Q, et al. Whole body vibration triggers a change in the mutual shaping state of intestinal microbiota and body's immunity. Front Bioeng Biotechnol. 2019;7. 10.3389/fbioe.2019.00377. [PubMed: 30733943]
65. Blanks AM, Rodriguez-Miguelez P, Looney J, et al. Whole body vibration elicits differential immune and metabolic responses in obese and normal weight individuals. Brain Behav Immun Health. 2020;1:100011. 10.1016/j.bbih.2019.100011. [PubMed: 38377415]
66. Hu KH, Butte MJ. T cell activation requires force generation. J Cell Biol. 2016;213(5):535–542. 10.1083/jcb.201511053. [PubMed: 27241914]
67. Rossy J, Laufer JM, Legler DF. Role of mechanotransduction and tension in T cell function. Front Immunol. 2018;9:2638. 10.3389/fimmu.2018.02638. [PubMed: 30519239]
68. Sen B, Xie Z, Case N, Ma M, Rubin C, Rubin J. Mechanical strain inhibits adipogenesis in mesenchymal stem cells by stimulating a durable beta-catenin signal. Endocrinology. 2008;149(12):6065–6075. 10.1210/en.2008-0687. [PubMed: 18687779]
69. Case N, Thomas J, Sen B, et al. Mechanical regulation of glycogen synthase kinase 3β (GSK3β) in mesenchymal stem cells is dependent on Akt protein serine 473 phosphorylation via mTORC2 protein. J Biol Chem. 2011;286(45):39450–39456. [PubMed: 21956113]
70. Yano S, Komine M, Fujimoto M, Okochi H, Tamaki K. Activation of Akt by mechanical stretching in human epidermal keratinocytes. Exp Dermatol. 2006;15(5):356–361. 10.1111/j.0906-6705.2006.00425.x. [PubMed: 16630075]
71. Kane LP, Andres PG, Howland KC, Abbas AK, Weiss A. Akt provides the CD28 costimulatory signal for up-regulation of IL-2 and IFN-gamma but not TH2 cytokines. Nat Immunol. 2001;2(1):37–44. 10.1038/83144. [PubMed: 11135576]

72. Appleman LJ, van Puijenbroek AA, Shu KM, Nadler LM, Boussiotis VA. CD28 costimulation mediates down-regulation of p27kip1 and cell cycle progression by activation of the PI3K/PKB signaling pathway in primary human T cells. J Immunol. 2002;168(6):2729–2736. 10.4049/jimmunol.168.6.2729. [PubMed: 11884439]

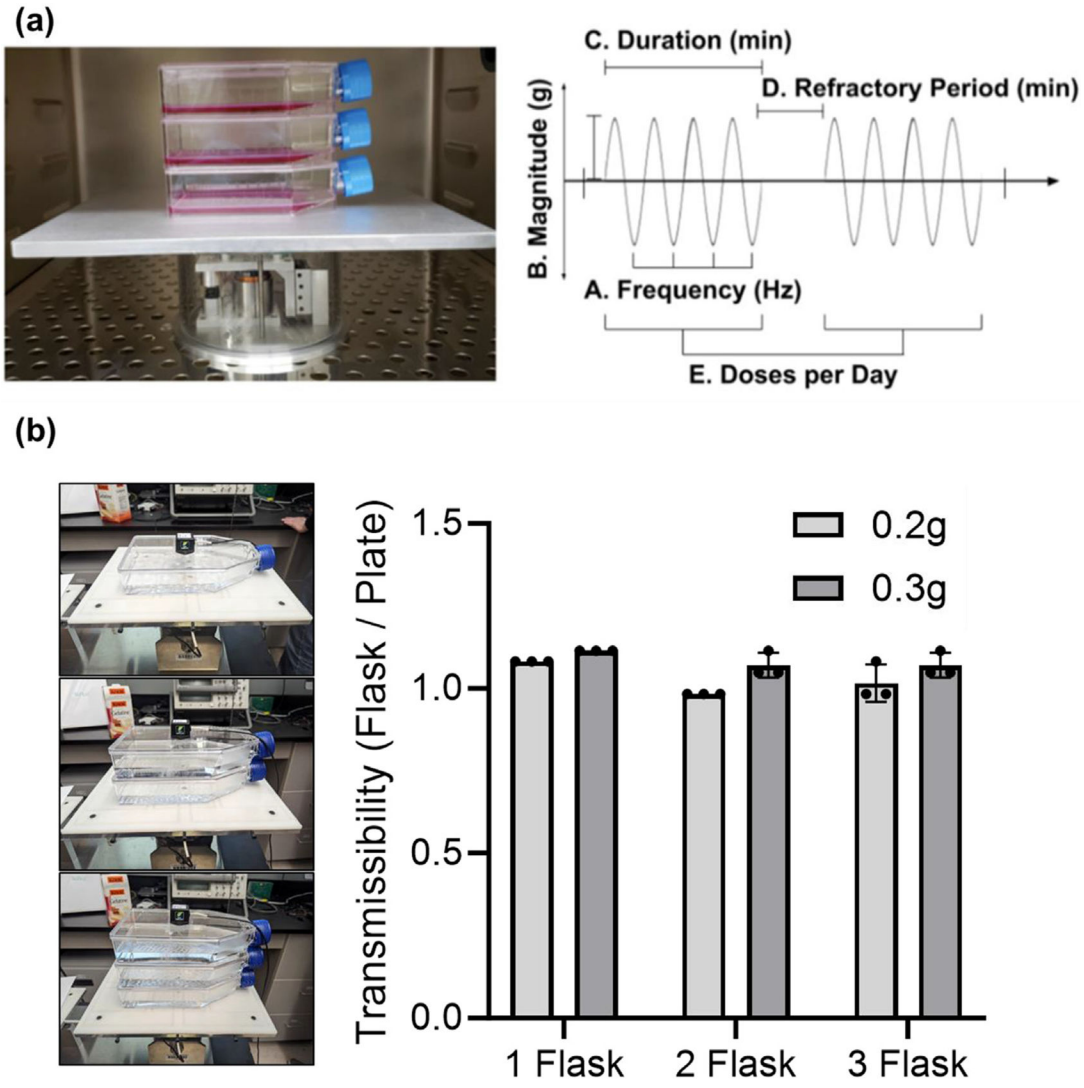

Fig. 1.

(a) LIV device pictured inside incubator with stacked T75 flasks on the top plate (left). Driving the platform is an electromagnetic actuator displacing in the vertical direction, with current regulated through closed-loop feedback as based on an accelerometer affixed to the bottom of the top plate. LIV parameters examined in these protocols (right) are customizable via LabView PID, and include magnitude, frequency, duration, refractory period and doses per day. (b) To test the transmissibility of the vibration signal on stacked flasks, single, two or three flask configurations were vibrated at 30 Hz with acceleration magnitudes of 0.2 g and 0.3 g. The vibration magnitude readings at the top of the flask were compared to a reference accelerometer attached to the vibrating platform. Transmissibility, defined as the ratio of reference plate acceleration to flask acceleration was calculated. Results show that transmissibility ratio was very close to 1 for each tested condition, showing that 100% of the signal was successfully transferred to stacked flasks. Experiments were repeated with three independent biological replicates, individual measurements were given on the graph.

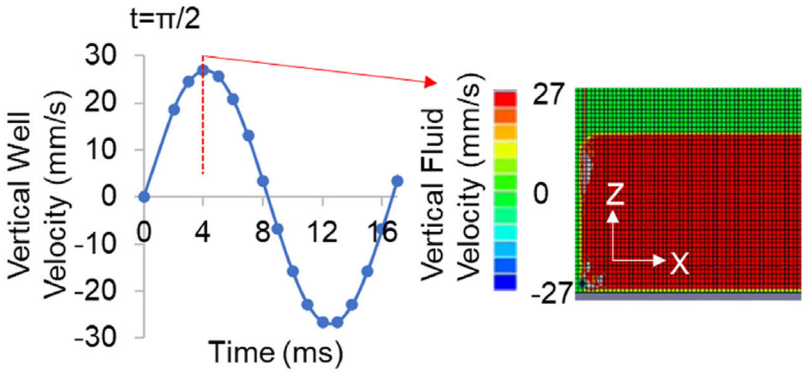

Fig. 2.

A finite element model was used to determine fluid motions in a vertical vibration of a 6-well plate (left). Peak out of plane strain(ε) during 2 cycles of 0.7 g, 90 Hz vertical vibration is shown in center. Fluid motion was modeled in Abaqus (6.9.1, Simula, RI). Vertical velocity distribution during t = π/2 shows that fluid motion was coupled to the vertical well peaking at 27 mm/s (right).

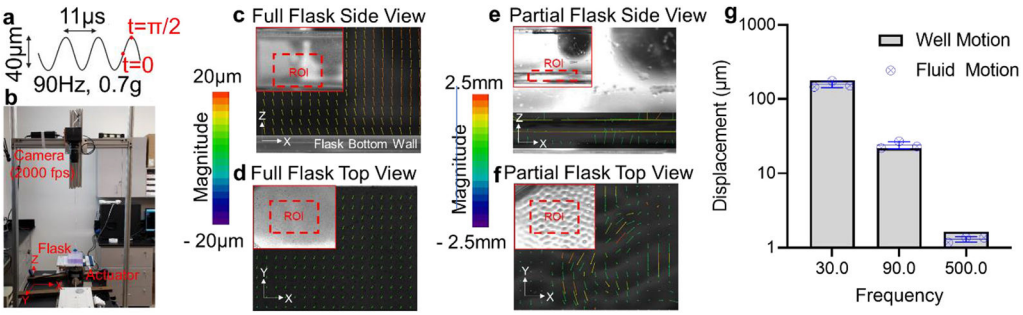

Fig. 3.

Fully or partially filled flasks were vibrated and fluid motions were quantified. (a) LIV was applied at 90 Hz and 0.7 g, generating peak motion of 20 μm per cycle. (b) A Photron UX50 high speed camera at a rate of 2000 frames per second recorded the fluid motion from either side view or top view during vertical vibration driven by a Labworks ET-126HF-1,-4 (13lbf) transducer using a sinusoidal driving function. Frames between t = 0 and t = π/2 that correspond to peak cycle displacement were compared within the region of interest (ROI, red bounding box) to determine the acceleration transmittance and fluid sloshing. (c) Side motion of the full flasks shown that fluid motion vectors were lined parallel to actuator motion with a maximum magnitude of 18 μm, essentially matching to the 20 μm peak motion of the actuator and (d) fluid sloshing measured from top view was minimal around 2 μm. (e) While displacement vectors from the side view of partially filled flasks showed peak motion at 2.5 mm – two orders of magnitude larger than filled flasks. (f) Similarly, fluid sloshing measured from top view showed large motions of unconstrained fluid motions peaking at magnitude of 2.5 mm. (g) Comparing the transmittance of 0.7 g acceleration magnitude in full flasks shows close to 100% transmittance across 30, 90 and 500 Hz frequencies. Data were generated from three different measurements, where each measurement was taken from a separate trial (n = 3 independent experiments).

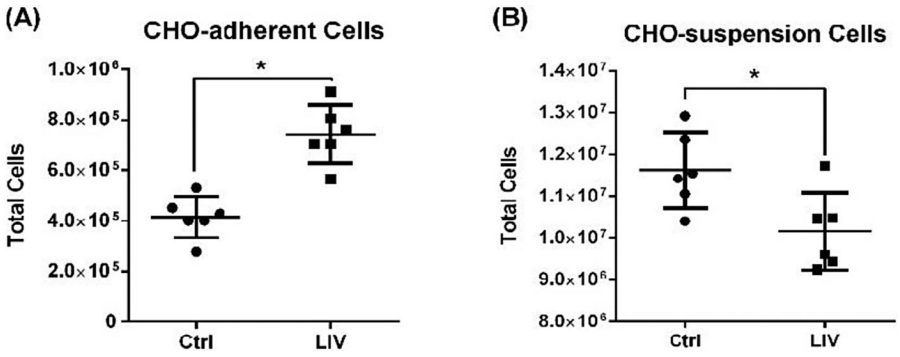

Fig. 4.

LIV signal of identical intensity, frequency, duration and refractory period (0.2 g, 500 Hz, 3 × 30 min/d, 2 hr refractory period) showed significant, but opposing, proliferative responses in (A) CHO-adherent cells (+79%) and (B) CHO-suspension cells (−13%) (n = 6 independent experiments per group, mean ± SD, $p \leq 0.05$).

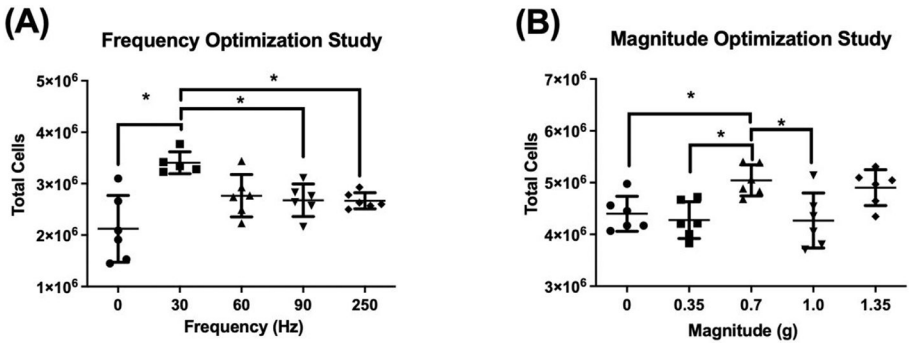

Fig. 5.

(A) Varying the LIV frequency applied to CHO-suspension cells showed a 61% increase at 30 Hz compared to control, significantly greater than 90 Hz or 250 Hz. (B) While at a fixed 30 Hz frequency, a 0.7 g magnitude was distinguished as more influential than other inputs with a 15% increase compared to control. (n = 6 independent experiments per group, mean ± SD, $p \leq 0.05$).

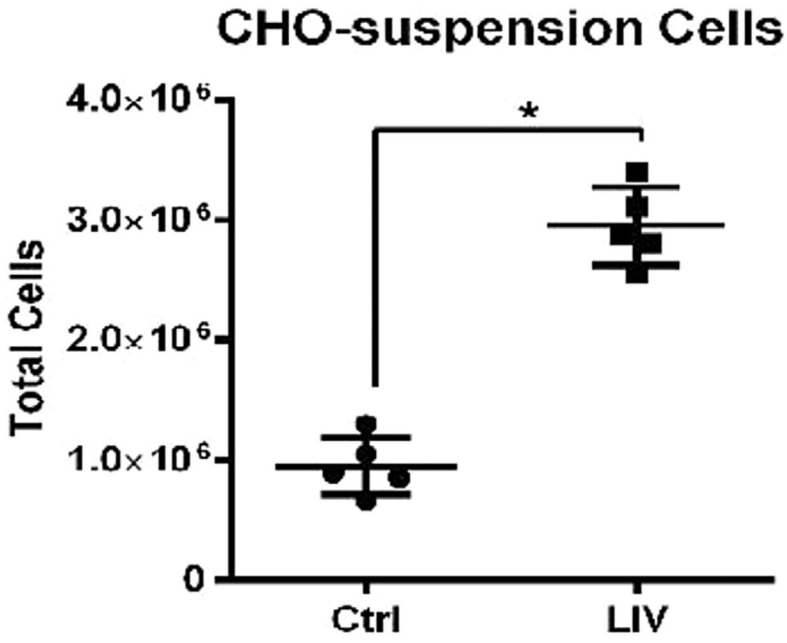

Fig. 6.

When subjected to same LIV protocol (30 Hz, 0.7 g, 2 bouts of 1 h/d, 2-h refractory period), CHO-Suspension cells resulted in a 210% increase in cell proliferation. (n = 5 independent experiments *$p < 0.05$ Data presented as mean ± SD).

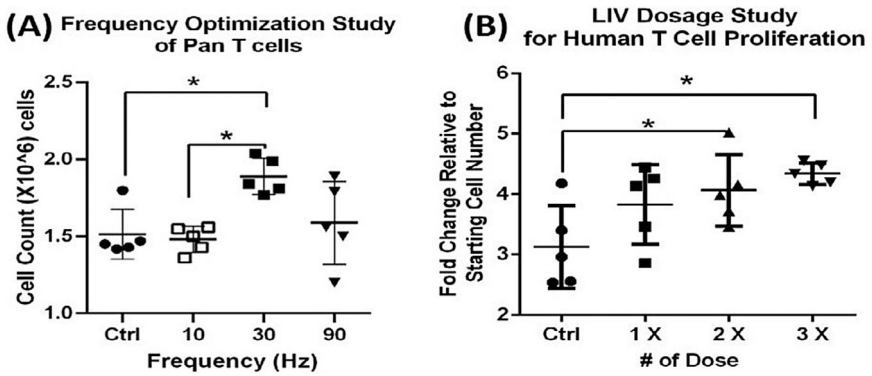

Fig. 7.

48-h frequency and dosage optimization experiment (A) human primary T cells exposed to LIV at 30 Hz showed an increase in proliferation of 24.8% as compared to sham controls ($n = 5$ independent experiments, mean, $P < 0.05$). (B) Increasing from 1 to 2 LIV doses elevated proliferation by 31% ($p < 0.05$), while 3 doses increased proliferation by 39% when compared to sham group ($p = 0.01$).

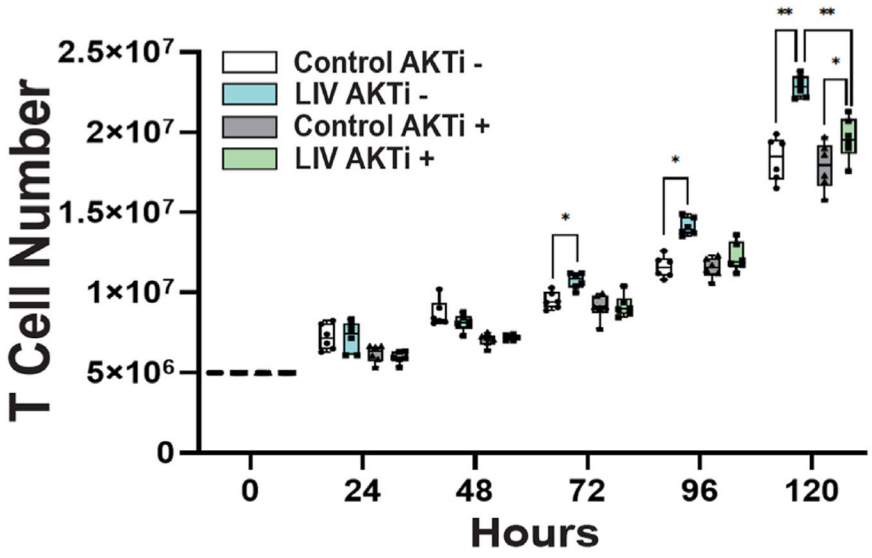

Fig. 8.

One set of control and LIV exposed cells was grown in the presence of the AKT inhibitor VIII (1uL/mL) Following 5 days exposure to LIV we found that cells grown without the AKT inhibitor LIV enhanced cell growth by 24% relative to controls (** = $p < 0.01$, n = 6 independent experiments). LIV exposed cells that were cultured with AKTi VIII only grew 9% more than their controls (* = $p < 0.05$, n = 6 independent experiments). Addition of AKTi VIII reduced the proliferative effect of LIV by 62%.